

The geometric phase of Z_n - and T-symmetric nanomagnets as a classification toolkit

M. Prada^{1,*}

¹*I. Institut für Theoretische Physik, Universität Hamburg, Jungiusstr. 9, 20355 Hamburg, Germany*

(Dated: May 10, 2022)

We derive the general form of the non-trivial geometric phase resulting from the unique combination of point group and time reversal symmetries. This phase arises *e.g.* when a magnetic adatom is adsorbed on a non-magnetic C_n crystal surface, where n denotes the fold of the principal axis. The energetic ordering and the relevant quantum numbers of the eigenstates are entirely determined by this quantity. Moreover, this phase allows to conveniently predict the protection mechanism of any prepared state, shedding light onto a large number of experiments and allowing a classification scheme. Owing to its robustness this geometric phase also has great relevance for a large number of applications in quantum computing, where topologically protected states bearing long relaxation times are highly desired.

I. INTRODUCTION

In the early 80's, Berry discovered an intriguing, non-integrable phase depending only on the geometry of the parametric space [1]. This phase, which had been overlooked for decades, provided a deep insight on the geometric structure of quantum mechanics, resulting in various observable effects. The concept of the Berry phase is a central unifying concept in quantum mechanics, shedding light onto a broad range of phenomena such as the Aharonov-Bohm effect, the quantum and the anomalous Hall effect, etc. Moreover, geometric or Berry phases nowadays represent the most robust resource for storing and processing quantum information [2].

In this work, we focus on the fundamental aspects of the geometric phase arising from the combination of n -fold (Z_n) point group and time reversal (TR) symmetries. This concept appears in a clean and illustrative form in spin adsorbates (SA) on non-magnetic crystal structures, with point group C_n while being time-reversal symmetric. SA such as magnetic adatoms or clusters, have recently attracted attention due to their potential application as a platform for quantum computing and high-density magnetic-based data storage [3–13], as well as for the study of fundamental phenomena such as the Kondo effect [14–18]. In these structures, the large magnetic moment of the SA adapts to the anisotropic crystal field, resulting in non-trivial spin dynamics and bearing enhanced lifetimes of the two degenerate ground states in the SA [19–22]. However, a general classification scheme of this novel symmetry combination has not been so far reported, nor a comprehensive study of the mechanisms responsible for this spin protection from a general perspective. Moreover, TR operation in these protected states has not been explored to its depth.

Here we derive an exotic geometric phase that captures all the possible symmetry combinations of a SA on a n -fold ($n = 2, 3, 4, 6$) surface at once. With only this quantity, a general classification scheme based purely on symmetry arguments follows. In addition, we obtain two quantum numbers resulting from the intriguing combination of the symmetries. Finally, we are able to predict the allowed transitions induced

by a general exchange interaction, finding topologically protected states for some particular symmetry and spin choices. This phase permits thus to deal with two related problems at once, both relevant to the use single quantized spins to store classical information: whether or not the ground state is doubly degenerate, and whether or not direct exchange-mediated spin transitions may occur between the two ground states. Hence, this phase may suggest novel designs of fault-tolerant, SA based quantum logic gates.

II. METHODS

For a free SA spherical symmetry exists, and the SA is characterized by a set of $(2J + 1)$ fully degenerate eigenstates, $\{|J, M\rangle\}$, where J denotes the 'spin', *e.g.* the effective spin \tilde{S} for transition metal ions, or the total angular momentum $L + S$ for rare earth ions, and M denotes its z -component. The symmetry is lowered when the SA is placed on an axially symmetric site, and it may be described by a generic axial term $\hat{H}_u = D\hat{J}_z^2$, resulting in a set of J pairs of states for J integer ($J + 1/2$, if half-integer). For transition metal (TM) ions, \hat{H}_u represents the axial zero field splitting term of an effective spin Hamiltonian, whereas for rare earths, \hat{H}_u is a physical crystal field Hamiltonian [23]. This occurs, for instance, in magnetic adsorbates on metallic substrates [17, 19, 22, 24]. For rhombic symmetry sites, a generic rhombic term \hat{H}_n must be added, which mixes the magnetic quantum numbers and hence M ceases to be a good quantum number. \hat{H}_n is a combination of n -powers of the ladder operators, [22, 25], $\hat{J}^\pm = \hat{J}_x \pm i\hat{J}_y$. To lowest order, the generic Hamiltonian for the SA reads:

$$\hat{H} = \hat{H}_u + \hat{H}_n = D_z(\hat{J}_z)^2 + E_n\{[(\hat{J}_+)^n + (\hat{J}_-)^n], \hat{J}_z^\alpha\}, \quad (1)$$

with $\{, \}$ denoting anticommutator. $\alpha = 0$ (1) for even (odd) n to ensure TR invariance of H [26]. The generic Hamiltonian in Eq. (1) can equivalently be expressed in terms of extended Stevens operators [27] $\hat{O}_k^q(\hat{X})$, with $\hat{X} = \hat{J}$ (in crystal field Hamiltonian, H_{CF}) or $\hat{X} = \hat{S}$ (in zero-field splitting Hamiltonian, H_{ZFS}) [28]. H_{ZFS} and H_{CF} in terms of Stevens operators possess identical mathematical structure and are subject to same symmetry constraints, however, their origin and meaning

* mprada@physnet.uni-hamburg.de

of ‘spin’ differ, bearing different parameter sets which should not be confused [23, 29, 30].

Without losing generality, we focus on the frequent (and experimentally relevant) case with $|D_z| \gg |E_n|$, $D_z < 0$, and $J > n$. By convention, the axes are assigned in Eq. (1) to maximize $|D_z|$, where the z -axis typically coincides with the many-fold normal to the crystal surface. Note that the crystal field potential reflects the point symmetry of the lattice site, and hence, it is written on its simplest form when the axes are the symmetry axes of the point group [31].

In order to find the relevant quantum numbers of the system, we consider the rotational and time-reversal symmetries associated with the point group of the crystal C_n and the absence of an external magnetic field, respectively,

$$[\hat{H}, \hat{R}_{2\pi/n}^z] = 0, \quad (2)$$

$$[\hat{H}, \hat{T}] = 0, \quad (3)$$

where we have defined the rotations of the C_n point group $\hat{R}_{2\pi/n}^z$, and the TR operator \hat{T} . The irreducible representation of the n -dimensional C_n group is given by $\{1, e^{i2\pi/n}, \dots, e^{i2\pi(n-1)/n}\}$, whereas the irreducible representation generated by TR has two elements, $\{1, -1\}$. As we will see below, a fundamental relative phase arises in a faithful representation that satisfies (2) and (3).

It appears natural to label the eigenstates according to the phase acquired under a $2\pi/n$ spin rotation, $2\pi m/n$ and the one related to the time-reversal operator, $\zeta(m, n)$. We stress that here we are introducing two new quantum numbers: m , arising from the discrete rotations of the C_n group, and $\zeta(m, n)$, describing the TR transformations. Considering first the rotations, we have

$$\hat{R}_{2\pi/n} |\Psi_m^\zeta\rangle = e^{i2\pi m/n} |\Psi_m^\zeta\rangle. \quad (4)$$

On what follows we choose m , an arbitrary representative of the rotational subgroup, to be the element with largest absolute value of z -component of the spin. We note that this rotationally invariant representation would correspond to the coloring code of the states commonly being used [22, 24, 32], and we want to point out its relation to the discrete $2\pi/n$ -rotations. E.g. Miyamachi *et al.* have $J = 8$ and $n = 3$, resulting in three rotationally invariant groups: one mixing $M = -8, -5, -2, 1, 4$, and 7 , (thus $m = -8$, usually marked ‘blue’ in literature), another mixing $M = -7, -4, -1, 2, 5, 8$ ($m = 8$, red), and the last one with $M = -6, -3, 0, 3, 6$ ($m = 6$, green). These corresponds to the irreducible representation $\{e^{i4\pi/3}, e^{i2\pi/3}, 1\}$, respectively, in terms of the phase each member of the subgroup acquires under the discrete rotations. This connection does not appear clear in the present literature. Finally, $|\Psi_m^\zeta\rangle$ is a linear combination of $|J, M\rangle$ states [25],

$$|\Psi_{\pm m}^\zeta\rangle = \sum_{|m-nk| \leq J} c_k^n |J, \pm(m-nk)\rangle. \quad (5)$$

c_k^m are some coefficients to be determined by the environmental field [29]. We may expect the largest contribution to the ground state to be given by $k = 0$ at $m = \pm J$. ζ labels the TR phase that connects two states in the time-reversed pair.

We now focus on the action of \hat{T} in (5):

$$\begin{aligned} \hat{T} |\Psi_m^\zeta\rangle &= \sum_{|m-nk| \leq J} (c_k^m)^* e^{i\pi(m-nk)} |J, -(m-nk)\rangle = \\ &= e^{i\pi m} \sum_{|m-nk| \leq J} (c_k^m)^* e^{-i\pi nk} |J, -(m-nk)\rangle. \end{aligned} \quad (6)$$

Applying the operator twice, \hat{T}^2 , we obtain the usual eigenvalues ± 1 (positive for integer m and negative, for m half-integer). However, noting the axial nature of spin, we have that $\hat{T} \hat{R}_{2\pi/n}^z = \hat{R}_{-2\pi/n}^z \hat{T}$, which involves that \hat{T} and $\hat{R}_{-2\pi/n}^z \hat{T} \hat{R}_{-2\pi/n}^z$ are two alternative ‘paths’ of the time reversal operator (see Fig. 1). Hence, the action of TR and this new ‘rotated time reversal’ (RTR) operator should yield the same state up to a global phase:

$$\begin{aligned} \hat{T}^- |\Psi_m^\zeta\rangle &\equiv \hat{R}_{-2\pi/n}^z \hat{T} \hat{R}_{-2\pi/n}^z |\Psi_m^\zeta\rangle = \hat{R}_{-2\pi/n}^z \hat{T} e^{-2i\pi m/n} |\Psi_m^\zeta\rangle \\ &= e^{i\pi m(1+2/n)} \hat{R}_{-2\pi/n}^z \sum_{|m-nk| \leq J} (c_k^m)^* e^{-i\pi nk} |J, -(m-nk)\rangle \\ &= e^{i\pi m(1+4/n)} \sum_{|m-nk| \leq J} (c_k^m)^* e^{-i\pi nk} |J, -(m-nk)\rangle, \end{aligned} \quad (7)$$

where we have named the ‘clockwise’ RTR operator \hat{T}^- . Likewise, we may define its counterpart: $\hat{T}^+ \equiv \hat{R}_{2\pi/n}^z \hat{T} \hat{R}_{2\pi/n}^z$, involving anti-clockwise rotations. It is straight forward to see that a global phase is obtained under the action of $(\hat{T}^-)^2$:

$$(\hat{T}^-)^2 |\Psi_m^\zeta\rangle = e^{2i\zeta} |\Psi_m^\zeta\rangle = e^{2i\pi m(1+4/n)} |\Psi_m^\zeta\rangle,$$

yielding

$$\zeta(m, n) = \pi m \left(1 + \frac{4}{n}\right). \quad (8)$$

Likewise, a phase $2\zeta'(m, n) = 2\pi m(1 - 4/n)$ is obtained by the action of $(\hat{T}^+)^2$, however these phases bear a similar classification scheme, as we will see below. Note that the action of subsequent (\hat{T}^-) and (\hat{T}^+) yields the usual Wigner’s phase, $2i\pi m$: $(\hat{T}^+)(\hat{T}^-) |\Psi_m^\zeta\rangle = e^{-i(\zeta'(m, n) - \zeta(-m, n))} |\Psi_m^\zeta\rangle = e^{-2i\pi m} |\Psi_m^\zeta\rangle$.

III. RESULTS AND DISCUSSION

Eq. (8) is the central result of this work, and can be identified with a geometric phase that arises due to the non-trivial TR and rotational symmetry combination. A graphical interpretation is given in Fig. 1: $\zeta(m, n)$ would be the phase acquired under a rotated time-reversal operation onto one of the states at the bottom of the zone (red path). This phase is topological in the sense that it can only be defined within the cyclic group C_n and the related closed paths in the Bloch sphere [33–35]. The states fold energetically in n -periodic subgroups, in a similar way as k -states in the different bands of a solid.

Noting that the choice of the representative is arbitrary, we choose on what follows m to take the largest positive value.

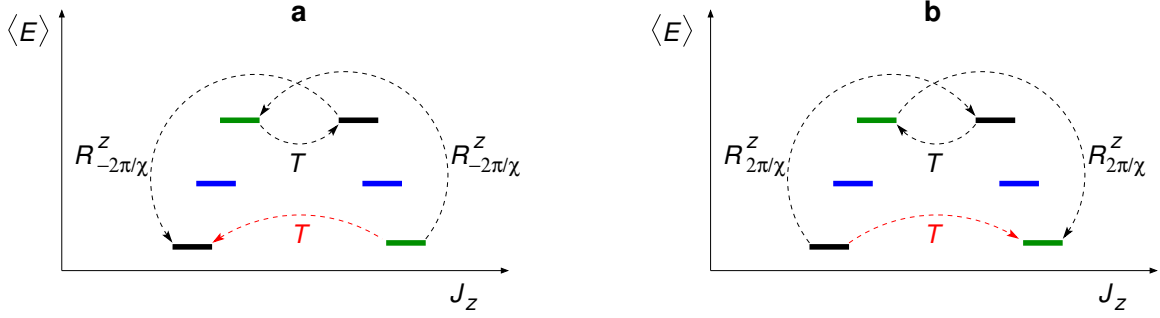


FIG. 1. Cartoon illustrating the two paths that connect time-reversed pairs for different J_z states: Direct time-reversal (red broken lines) and rotated time reversal \hat{T}^+ and \hat{T}^- (black broken lines in a and b, respectively). Note that J_z is *not* a good quantum number, and hence the symbols do not represent eigenstates: The vertical axis correspond to the mean value of the energy (not to scale).

Every pair of states $|\psi_{\pm m}^{\zeta(\pm m, n)}\rangle$ can be thus connected under RTR symmetry by a complex number with phase $i\zeta(m, n)$, hence real (or integer) RTR-statistics whenever $\zeta(m, n)$ is an integer multiple of π . In view of (8), the RTR character of the original SA may switch in the presence of an environmental field: For integer J , is easy to see that $\zeta(m, n)/\pi$ is fractional if $4m/n$ is a fractional number. In this case, we obtain a complex phase under RTR (this occurs, for instance, in the GS pair of Ho impurities in 3-fold crystals, $m = \pm 8$, $n = 3$ [22]). However, for half-integer J , we have that $\zeta(m, n)/\pi$ may be integer for $(n+4)/n$ even, occurring for $n = 4$ and any J (half-integer). Table I lists all the possible eigenvalues of the time-reversed pair of \hat{R} and related TR phases, for any combination of m and n .

For completeness, we evaluate next the possible protection mechanisms to first order based on the values of table I, allowing us to obtaining a general classification scheme. In general, the experimental setups designed for memory storage aim for a magnetic ground state as robust (or long lived) as possible. Hence, it appears relevant to study the protection to zero-th order [12, 37], by examining $\langle \psi_m^{\zeta(m)} | \psi_{-m}^{\zeta(-m)} \rangle$. It is immediate to see that the pair is actually the *same* state when both m and $2m/n$ are integers. The latter condition indicate that they are the same rotational class, whereas the former leads to a real representation of the time-reversal group ($i\zeta_m$ is then an integer multiple of $i\pi$). In addition, a coefficient relation may easily be obtained, using (6) in (5):

$$c_k^m = e^{i\pi nk} (c_k^{-m})^*. \quad (9)$$

In terms of the original components, the crystal Hamiltonian H_n mixes $|J, \pm M\rangle$ and $|J, \pm(M - nk)\rangle$. Together with (9), and choosing the coefficients c_k^m to be real, this implies non-magnetic ($\langle \hat{J}_z \rangle = 0$) bonding and anti-bonding mixtures, commonly termed as quantum spin tunneling splitting [25]. This brings two consequences: (i) if $m = \pm J$, then preparation of a magnetic ground state would result into short relaxation times [22] and quantum spin tunneling [16] (ii) if $m \neq J$, this results in the appearance of a shortcut tunneling [22, 24]. We stress that we do not attempt in this work to quantitatively predict the relaxation of a magnet, but rather predict and classify the emerging states by symmetry arguments.

In typical samples, the main mechanism for magnetization

reversal are spin-flip events mediated by exchange interaction with substrate or tunneling electrons [24, 38–42], which can be described in its most general form, as

$$\hat{H}_e = \alpha \hat{J} \cdot \hat{\sigma},$$

where σ_i are the usual Pauli matrices denoting the electronic spin and α is an arbitrary constant. In the weak coupling limit, the degrees of freedom of the electrons and the adatom factorize, and we may consider the matrix element $\langle \psi_m^{\zeta(m)} | \hat{J} | \psi_{-m}^{\zeta(-m)} \rangle$. Using the anti-unitarity of the TR operator and Eq. (7), we have

$$\begin{aligned} \langle \psi_m^{\zeta(m)} | \hat{J} | \psi_{-m}^{\zeta(-m)} \rangle &= \langle \hat{T}^+ \psi_m^{\zeta(m)} | \hat{T}^+ \hat{J} (\hat{T}^+)^{-1} | \hat{T}^+ \psi_{-m}^{\zeta(-m)} \rangle^* = \\ &= -\langle \hat{T}^+ \psi_m^{\zeta(m)} | \hat{J} | \hat{T}^+ \psi_{-m}^{\zeta(-m)} \rangle^* = \\ &= -e^{-2i\zeta(m)} \langle \psi_m^{\zeta(m)} | \hat{J} | \psi_{-m}^{\zeta(-m)} \rangle. \end{aligned} \quad (10)$$

We stress the importance of the phase $\zeta(m)$, since the matrix element may exist only when (i) $2i\zeta(m) = i\pi(2l+1)$, $l \in \mathbb{Z}$, and (ii) $-m+1$ and m (or $-m-1$ and $-m$) belong to the same class, or equivalently, when (i) $2m(1+4/n)$ is an *odd integer* and (ii) $(2m-1)/n$ [or $(2m+1)/n$] is an *integer*.

For the former, (i), we would like to stress that a complex phase different to $2i\zeta(m) = i\pi$ forces the matrix element in Eq. (10) to be 0, which we will term as time-reversal protection. A geometrical interpretation of this cancellation was already noted by von Delft *et al.* [34], where the topological phase leads to destructive interference between the symmetry-related tunneling paths. Although not affecting the overall results in the particular case studied by [22, 32], we want to note that this phase was not taken into account by Miyamachi *et al.* nor by Karlewski *et al.* yielding a difference between our Eq. (10) and Eq. (4) in [22] or Eq. (6) in [32]]. Hence, this phase delivers naturally the correct classification scheme.

Condition (ii), on the other hand, tells us that the matrix element vanishes if the states belong to different rotational class, and hence, these would be protected by rotational symmetry. Note that one could have considered the matrix element $\langle \psi_m^{\zeta(m)} | \hat{J}_z | \psi_{-m}^{\zeta(-m)} \rangle$ in half-integer J case, requiring that m and m belong to the same class. This implies $2m/n$ integer, which could only happen for $n = 3$. However, $\zeta(m)$ differs always

TABLE I. List of all possible $\hat{R}\hat{T}\hat{R}$ -related phases, $e^{i\zeta}$ (upper rows) and \hat{R} eigenvalues, $e^{i2\pi/n}$ (lower rows), for any n and m combination. $I =$ integer m , $HI =$ half-integer m .

Symmetry, m		$n = 2$	$n = 3$	$n = 4$	$n = 6$
\hat{T}	I	± 1	$\pm 1, e^{\pm i\pi/3}, e^{\pm 2i\pi/3}$	+1	$\pm 1, e^{\pm i\pi/3}, e^{\pm 2i\pi/3}$
	HI	$e^{\pm i\pi/2}$	$e^{\pm i\pi/6}, e^{\pm i\pi/2}, e^{\pm 5i\pi/6}$	-1	$e^{\pm i\pi/6}, e^{\pm i\pi/2}, e^{\pm 5i\pi/6}$
\hat{R}	I	± 1	$1, e^{\pm 2i\pi/3}$	$\pm 1, e^{\pm i\pi/2}$	$\pm 1, e^{\pm i\pi/3}, e^{\pm 2i\pi/3}$
	HI	$e^{\pm i\pi/2}$	$-1, e^{\pm i\pi/3}$	$e^{\pm i\pi/4}, e^{\pm 3i\pi/4}$	$e^{\pm i\pi/6}, e^{\pm i\pi/2}, e^{\pm 5i\pi/6}$

from $\zeta(-m)$ in this case, making the matrix element vanish (see yellow pairs in fig. 2 d).

Based on the above, we may draw a few conclusions: (i) when both m and $2m/n$ are integers, we expect non-magnetic energy split states. Otherwise, the pair of states remain degenerate. (ii) The ground states are protected by both, TR and rotational symmetry for integer J and fractional $2J/n$: the latter implies that they belong to different rotational classes. One may expect a more robust protection if $(2J - 1)/n$ is also fractional by employing a similar argument. (iii) The ground states are protected by TR for a fractional J to zero order, even if $2J/n$ is integer, and further, if $(2J - 1)/n$ is fractional, then symmetry protection appears to first order. Finally, (iv) the ground states are protected by TR symmetry for fractional J and fractional $2J/n$. In this last case, if $(2J - 1)/n$ is 0 or integer, then the protection is exclusively by TR, and we may say the states are *topologically protected*. This topologically protected states may occur for $n = 3, 6$ and $m = 1/2, 7/2, \dots (1 + 6k)/2$, with k integer, and $n = 4$ and $m \neq 5/2, 11/2, \dots (1 + 4k)/2$, with k integer.

The ordering of the lowest n pairs ($2n$ pairs, for $n = 3$) is depicted in Fig. 2, as a function of the phase $\zeta(m)$ defined in (8). Assuming $|D_z| > E_n$ and $J > n$, the uniaxial term dominates, and thus we may expect the energy levels to be determined by m . The left panels (a,c,e,g) correspond to integer J , whereas the right ones (b,d,f,h) belong to half-integer J . For each case we consider only the first n pairs of states, hence from $m = \pm J$ to $m = \pm(J - n)$. These describe the first fold, pretty much like the k -states in a Brillouin zone. In fact, higher energy states will then acquire similar discrete phases. Note that the ordering of the states could be altered when considering higher order terms, whereas truncation of the fourth-rank ($k = 0$) terms may introduce errors [31, 43]. However, for the sake of simplicity, we restrict our discussion to the Hamiltonian defined in (1). The labels (PT, PP, K, T) describe the protection of each pair, assuming the pair is at the ground state.

For $n = 2$ (upper panels of Fig. 2), noting that $2m/n = m$ is integer (fractional) whenever m is (semi-)integer, we conclude that the two states always belong to the same (different) rotational class. For integer m , there is only one possibility, which is the non-magnetic combinations of states, commonly termed as the tunneling case (T) [16]. The symmetry rotation yields a real eigenvalue, 1 (black) or -1 (yellow). However, for half-integer m , the two conditions for exchange mixing $2i\zeta(m) = i\pi(2l + 1)$, $l \in \mathbb{Z}$, and integer $(2m \pm 1)/n$ are both satisfied, allowing exchange mixing of the pair. This is the so-called Kondo (K) case, where scattering with a single electron leads to transitions between the two ground states. Note

that the eigenvalue of the rotations is complex $e^{\pm i\pi/2}$, where the sign alternates on each level (light and dark green) and it coincides with the eigenvalue of \hat{T}^{\pm} .

For $n = 3$ (panels c, d of Fig. 2), we have three possible phases, which are again different for m integer or half-integer. For the former case, $2m/n$ is only integer for m multiple of 3, which implies a real $e^{i\zeta(m)}$. Those are the split states (black, rotation eigenvalue = 1) already noted in the panel above (T). When $2m/3$ is fractional, however, the time-reversed states can be related by a complex phase of $\pm\pi/3$ or $\pm 2\pi/3$, which can have a rotational phase of $2\pi/3$ or $-2\pi/3$. Those are the brown and red colored states. If the next level is the split pair, then the pair is protected by both point group and TR symmetry (PP,PT). However, if the next pair contains the same rotational classes, then the single electron scattering mechanism is still unavailable, since $2\zeta(m, n = 3)$ is fractional (see Eq. (10)), bearing a cancellation by topologically protected states. For the half-integer J , $n = 3$ case, $e^{i\zeta(m, n = 3)}$ is always complex, implying that Kramers theorem applies for all states. Hence, when the pair belongs to the same rotational class, neither direct mixing nor exchange mixing may occur. We may then say that the states are protected by TR (yellow pair of Fig. 2.d). Finally, a set of states are protected only by time reversal (labeled PT), for which the state right above is of the same rotational class, yet the first order transition would be forbidden by time-reversal. We conclude that for the $n = 3$ half-integer J case, transitions to the time-reversed state would involve at least second order processes, see Fig. 2d.

For $n = 4$, $i\zeta(m) = 2i\pi m$. With the restriction $-\pi < \zeta(m) \leq \pi$, all states fall in phase zero (π) for integer m (half-integer m). It is easy to see that if m is an even integer, then the pair is in the same rotational class, resulting in the splitting (T), whereas an odd integer m results in protected states also under exchange with electrons: the rotational phases of the pair are $\pm\pi/2$. This results in the alternating pattern of Fig. 2e. In the half-integer case, none of the conditions for exchange with electrons $2i\zeta(m) = i\pi(2l + 1)$, $l \in \mathbb{Z}$ or $(2m - 1)/n$ integer are satisfied, bearing both PT and PP for all levels. Note that two levels of different rotational class (either $\pm\pi/4$ or $\pm 3\pi/4$) appear always degenerate in this case.

Finally, for $n = 6$ (panels g, h of Fig. 2), six different rotational classes appear, resulting in enhancement of the protection of the states. First order exchange with electrons is always forbidden, so the Kondo case is absent. For half-integer J , the protection is to highest order of all the possible cases, with all levels having at least PT: hence, the most robust protection would correspond to a SA with half integer J on a six-fold

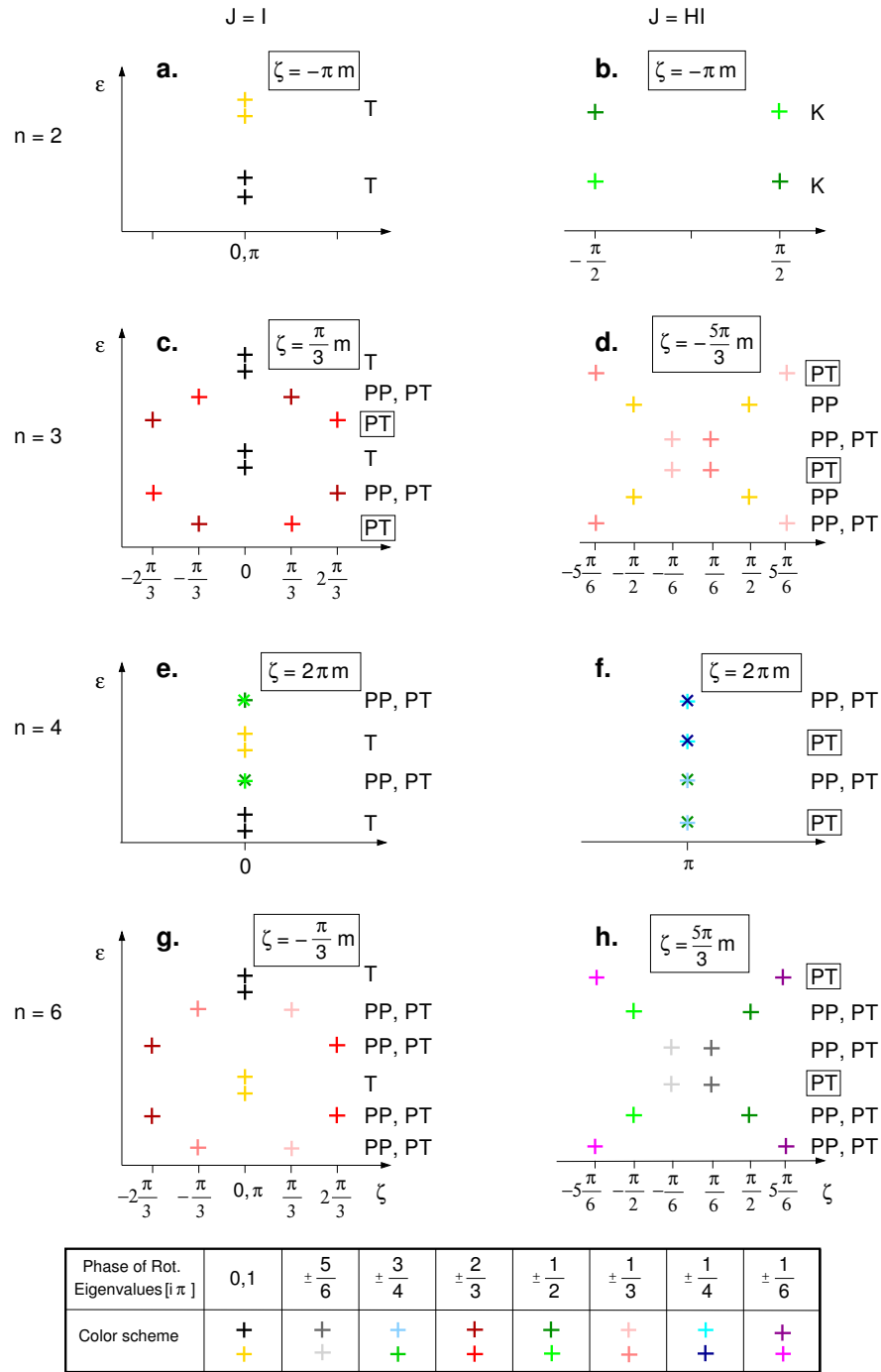


FIG. 2. Schematic representation of the lowest energy levels (not to scale) for each J, n possible combination as a function of the time reversal phase defined in (8), $\zeta(m)$, whose m dependency is given at the top of each figure. The different cases are labeled according to four different scenarios, T = tunneling, K = Kondo, PP = Protected by point-group, PT = Protected by time reversal. For the cases where only PT is available, the states are topologically protected (signaled by a boxed ‘PT’). The scenario of a given m depends on the characters of the pair, $-m$, and on the next excited state. Different colors labels the different rotational classes (see inset below) and symbols only change whenever a pair of states have the same phase $\zeta(m)$, for clarity.

crystal field.

Note that the theory presented here applies as well for $J \leq n$, only that in this case not all the states of Fig. 2 would enter the diagram. For instance, if we consider $J = 3/2$ and $n = 6$, only

the four topmost states depicted in Fig. 2h would appear. A generalization to the case where the GS is not dominated by $M = \pm J$ is possible with some modifications. Although the same phase spectrum $\zeta(m)$ would be observed, the energetic

ordering would change and also the evaluation of the matrix elements in (10) would need to be re-adapted.

IV. CONCLUSIONS

We have derived the quantum numbers that describe the discrete rotations of a SA on a non-magnetic substrate with a n -fold rotational axis. The point group symmetry in combination with time reversal symmetry yield a non-trivial topological phase, revealing the intriguing protection mechanisms of the resulting ground states, associated to a rotated time reversal operator. We have developed a comprehensive classifica-

tion scheme based solely on symmetry arguments, which reveals a particular folding of states. Our results are relevant for the proposal of SA-based memory storage devices, as well as for the recent studies revealing Kondo effect in SA. Moreover, our findings should stimulate experimental groups to find interferometry experiments that allow to unveil this geometric phase [2].

Acknowledgments:

We thank D. Pfannkuche, C. Hübner, A. Chudnovskiy and O. Tchernyshyov for valuable discussions. We acknowledge support of this work by the Deutsche Forschungsgemeinschaft (Germany) within SFB 925 and GrK 1286.

-
- [1] M. V. Berry, *Proc. R. Soc. Lond. A*, **392**, 45–57 (1984).
- [2] C. G. Yale, F. J. Heremans, B. B. Zhou, A. Auer, G. Burkard and D. D. Awschalom, *Nature Photon.* doi:10.1038/nphoton.2015.278 (2016)
- [3] R. Vincent, S. Klyatskaya, M. Ruben, W. Wernsdorfer, and F. Balestro, *Nature* **488**, 357 (2012);
- [4] B. W. Heinrich, L. Braun, J. I. Pascual and K. J. Franke, *Nature Phys.* **9**, 765–768 (2013);
- [5] I. Fernández-Torrente, D. Kreikemeyer-Lorenzo, A. Stróżecka, K. J. Franke, and J. I. Pascual, *Phys. Rev. Lett.* **2012**, 108, 036801.
- [6] S. Thiele, F. Balestro, R. Ballou, S. Klyatskaya, M. Ruben, and W. Wernsdorfer, *Science* **344**, 1135 (2014).
- [7] J. Parks *et al.* *Science* **328**, 1370 (2010).
- [8] S. Loth, S. Baumann, C. P. Lutz, D. M. Eigler, and A. J. Heinrich, *Science*, **335**, 196–199 (2012).
- [9] A. Stróżecka, M. Soriano, J. I. Pascual, and J. J. Palacios, *Phys. Rev. Lett* **109**, 147202 (2012).
- [10] G. Christou, D. Gatteschi, D. N. Hendrickson, and R. Sessoli, *MRS Bulletin* **25**, 66–71 (2000).
- [11] I. G. Rau, *et al.*, *Science*, **344**, 988 (2014).
- [12] F. Delgado and J. Fernandez-Rossier, *Phys. Rev. Lett.*, **108**, 196602 (2012).
- [13] F. Donati *et al.*, *Science*, **352**, 318 (2016); S. Baumann *et al.*, *Science*, **350**, 417 (2015).
- [14] M. Ternes, A. J. Heinrich and W.-D. Schneider, *J. Phys.: Condens. Matter*, **21**, 53001 (2009).
- [15] I. Fernández-Torrente, K. J. Franke, J. I. Pascual, *Phys. Rev. Lett.*, **101**, 217203, (2008). K. J. Franke, G. Schulze, J. I. Pascual, *Science* **332**, 940 (2011). A. F. Otte *et al.*, *Nature Phys.* **4**, 847 (2008). A. F. Otte *et al.*, *Phys. Rev. Lett.* **103**, 107203 (2009).
- [16] F. Delgado, S. Loth, M. Zielinski, and J. Fernandez-Rossier, *EPL* **109** 57001 (2015).
- [17] J. -P. Gauyacq, N. Lorente, and F. D. Novaes, *Prog. Surf. Sci.* **87**, 63 (2012).
- [18] M. Ternes, *New J. Phys.* **17**, 063016 (2015).
- [19] C. F. Hirjibehedin, C.-Y. Lin, A. F. Otte, M. Ternes, C. P. Lutz, B. A. Jones, and A. J. Heinrich, *Science* **317**, 1199 (2007);
- [20] A. A. Khajetoorians, S. Lounis, B. Chilian, A. T. Costa, L. Zhou, D. L. Mills, J. Wiebe, and R. Wiesendanger, *Phys. Rev. Lett.* **106**, 037205 (2011);
- [21] T. Balashov, T. Schuh, A. F. Takacs, A. Ernst, S. Ostanin, J. Henk, I. Mertig, P. Bruno, T. Miyamachi, S. Suga, and W. Wulfhekel, *Phys. Rev. Lett.* **102**, 257203 (2009).
- [22] T. Miyamachi *et al.*, *Nature*, **503**, 242–246 (2013), Suppl. material, doi:10.1038/nature12759
- [23] C. Rudowicz, *Magn. Res. Rev.* **13**, 1 (1987); C. Rudowicz, and S. K. Misra, *Applied Spectroscopy Reviews* **36**, 11 (2001); C. Rudowicz, and M. Karbowski, *Coordination Chemistry Reviews*, **287**, 28 (2015).
- [24] C. Hübner, B. Baxevanis, A. A. Khajetoorians, and D. Pfannkuche, *Phys. Rev. B*, **90** 155134, (2014).
- [25] D. Gatteschi, R. Sessoli, J. Villain, *Molecular nanomagnets*, Oxford University Press, New York (2006).
- [26] T. Schuh *et al.*, *Phys. Rev. B* **84** 104401 (2011).
- [27] C. Rudowicz, C. Y. Chung, *J. Phys.: Condens. Matter* **16**, 1 (2004).
- [28] B. G. Wybourne, *Spectroscopic Properties of rare earths*, Wiley (1965); J. M. D. Coey, *Magnetism and magnetic materials*, Cambridge University Press (2009).
- [29] S. K. Misra, C. P. Poole, and H. Farach, *Appl. Magn. Reson.* **11**, 29 (1996).
- [30] C. Rudowicz and M. Karbowski, *Physica B* **451**, 134 (2014) & *Physica B* **456**, 330 (2015); C. Rudowicz, *Physica B* **403**, 1882 & **403**, 2312 (2008).
- [31] F. Donati *et al.*, *Phys. Rev. Lett.*, **113**, 237201, (2014), & Suppl. material.
- [32] C. Karlewski, *et al.* *arXiv, preprint arXiv:1502.02527* (2015).
- [33] D. Loss, D. P. DiVincenzo, and G. Grinstein, *Phys. Rev. Lett.*, **69** 3232, (1992); A. Shapere, and F. Wilczek, "Geometric phases in physics Advances Series in Mathematical Physics, Vol. 5, (1989).
- [34] J. von Delft, and C. L. Henley, *Phys. Rev. Lett.*, **69** 3236, (1992).
- [35] If we consider a pair of states labelled $\pm m$ in Eq. (5), the difference of the Euclidean action along two symmetry related paths connecting the pair, as derived by J. von Delft *et al.* [34], reduces to $(S^0 - S^m) \propto i4\pi m/n$. This results in a coherent path integral for the tunneling amplitude connecting the pair that is non-zero only if $2m$ is an integer multiple of n . We may thus conclude that Eq. (9) represents a topological phase.
- [36] H. Kramers, *Proc. of Koninklijke Akademie van Wetenschappen*, 959–972 (1930); H. Kramers, *Proc. Amsterdam Acad.* **33**, 959 (1930).
- [37] C. Romeike, M. R. Wegewijs, W. Hofstetter, and H. Schoeller, *Phys. Rev. Lett.* **96**, 196601 (2006).
- [38] N. Lorente, and J.-P. Gauyacq, *Phys. Rev. Lett.*, **103** 176601, (2009).
- [39] F. Delgado, J. J. Palacios, and J. Fernández-Rossier, *Phys. Rev. Lett.*, **104**, 026601 (2010).

[40] J. C. Oberg, *et al.*, *Nature Nanotechnology* **9**, 6468 (2014).
[41] A.A. Khajetoorians, *et al.*, *Science*, **339**, 55 (2013).

[42] A. Chudnovskiy, C. Hübner, B. Baxevanis, D. Pfannkuche, *Phys. Status Solidi B*, 113 (2014).
[43] C. Rudowicz, *J. Mag. Magn. Mat.*, **321**, 2946 (2009). C. Rudowicz, D. Piwowarska, *Solid State Commun.*, **151**, 855 (2011).